www.czasopisma.pan.pl PAN www.journals.pan.pl

Metrol. Meas. Syst., Vol. XXI (2014), No. 3, pp. 509–520.

PAN POLSKA AKADEMIA NAUK

METROLOGY AND MEASUREMENT SYSTEMS

Index 330930, ISSN 0860-8229

www.metrology.pg.gda.pl

M&MS

THE IMPEDANCE MEASUREMENTS PROBLEM IN ANTENNAS FOR RFID TECHNIQUE

Piotr Jankowski-Mihułowicz, Grzegorz Pitera, Mariusz Węglarski

Rzeszów University of Technology, Faculty of Electrical and Computer Engineering, Department of Electronic and Communications Systems, Pola 2, 35-959 Rzeszów, Poland (✉ pjanko@prz.edu.pl, http://pjanko.sd.prz.edu.pl, +48 17 854 4708*)*

Abstract

The authors paid particular attention to the problem of antenna impedance measurements in the RFID technique. These measurements have to be realized by using two ports of a vector network analyzer and dedicated passive differential probes. Since the measurement process and estimated parameters depend on the frequency band, operating conditions, type of the system component and antenna designs used, appropriate verification of the impedance parameters on the basis of properly conducted experiments is a crucial stage in the antenna synthesis of transponders and read/write devices. Accordingly, a systematized procedure of impedance measurements is proposed. It can be easily implemented by designers preparing antennas for different kinds of RFID applications. The essence of indirect measurements of the differential impedance parameters is discussed in details. The experimental verification has been made on the basis of a few representative examples.

Keywords: RFID, antenna, impedance measurement, differential probe.

1. Introduction

The Radio Frequency Identification (RFID) technique is being used increasingly in automated processes of object identification [1]. It is especially developed in various areas of people's economical and social activities, e.g. industry, consumer market, science, medicine, logistics and many other fields [2–5].

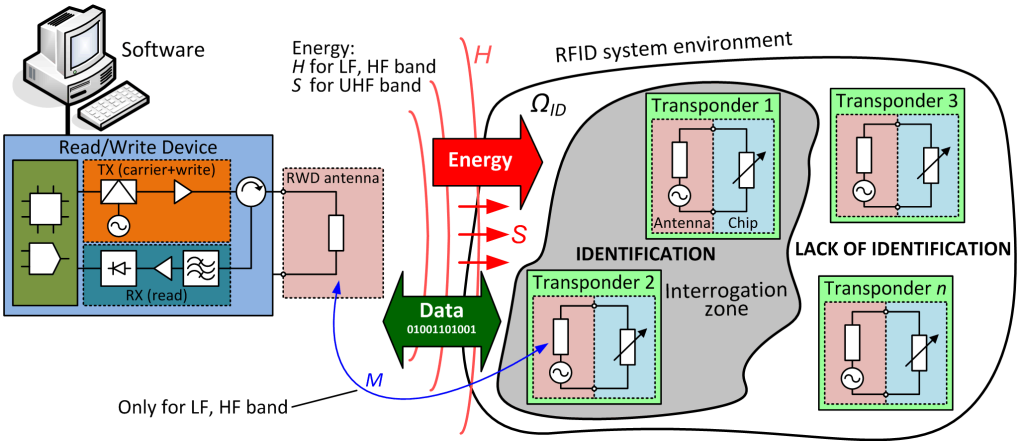

Fig. 1. Generalized block diagram of an RFID system.

Article history: received on Jan. 02, 2014; accepted on May. 05, 2014; available online on Sep. 15, 2014; DOI: 10.2478/mms-2014-0043.

A typical RFID system consists of transponders which are used for marking objects, and also a read/write device (RWD) and its antenna which form a management centre (Fig. 1). The operational capability of RFID systems is characterized by the interrogation zone (IZ) which is estimated in any direction of 3D space (Ω_{ID}) taking into account the changing localizations of activated transponder/transponders. The IZ parameter covers problems of energy and communication activity of all parts of the system arrangement. It also determines and comprehensively describes the possibilities of application of an RFID system in desirable automated processes. Moreover, on the basis of this parameter, it is possible to build a knowledge base about essential properties (parameters) of RFID equipment (transponders, RWD and its antenna).

It should be noted that many parameters and phenomena describing RFID systems have to be considered in a different way than it is in the classical theory of typical radio communication systems. For this reason, the authors paid particular attention to the problem of antenna impedance measurements. These measurements in a RFID application have to be realized by using two ports of a Vector Network Analyzer (VNA) and dedicated Passive Differential Probe (PDP). Since the measurement process and estimated parameters depend on the frequency band (LF/HF/UHF), operating conditions, type of the element (transponder/RWD) and antenna designs used, the appropriate verification of the impedance parameters on the basis of properly conducted experiments is a crucial stage in the antenna synthesis of RFID transponders and RWDs. It should be emphasized that precise values of antenna parameters are essential for estimating the main parameter – interrogation zone – describing a RFID system in its target application and also that the interrogation zone is very sensitive to errors made at the antenna design stage [6].

The usefulness of the RFID technique is determined by the possibility of its implementation to a particular situation and designed system efficiency in operational conditions. This can be predicted using the above-mentioned knowledge basis of system parameters.

2. Measurement problem

According to the main classification of RFID systems it is possible to distinguish applications operating in the inductive or radiative coupling regime. In the first group, the carrier frequency is between 100 kHz and 135 kHz (typically 125 kHz) for the LF band or 13.56 MHz in the HF band whereas in the second group – from 860 MHz to 960 MHz (UHF band), depending on the region of the world [1].

The inductive coupled systems operate by utilizing a zone that is characterized by an inhomogeneous magnetic field (characterized by the magnetic field strength H – Fig. 1) and strong coupling (characterized by the mutual inductance M – Fig. 1) between antennas of the arrangement components. For the typical operating frequency f_0=125 kHz in the LF band the wavelength λ is 2400 m and for f_0=13.56 MHz in the HF band λ is about 22 m. For this reason, the RWD and transponder antennas are made in the form of a loop which is small in relation to λ (Fig. 2). The inhomogeneous magnetic field generated in the RWD antenna vicinity is a medium for both energy transfer and wireless communication. The communication mechanisms are implemented in adequate protocols (for the LF band: UNIQUE, HITAG, TIRIS, for the HF band: ISO/IEC 15693, ISO/IEC 14443, ISO/IEC 18000-3 and others).

During antenna synthesis (for both components: transponders and RWDs) in the inductively coupled systems, the measurement problem is mainly related to determining parameters of a symmetrical (with respect to ground) antenna loop with an impedance Z_L

Metrol. Meas. Syst., Vol. XXI (2014), No. 3, pp. 509–520.

which is different from the typical value of 50 Ω. This impedance can be expressed by the formula:

$$Z_L = R_S + j\omega L_S , \tag{1}$$

where: R_S and L_S denote the series resistance and inductance of the loop antenna, $\omega=2\pi f_0$ describes the pulsation.

Correct specification of the loop parameters has a significant influence on next stages of the synthesis. In the RWD, the results are necessary for the design and construction of an impedance matching circuit [7–11] whereas in the transponders – for determining the parallel resonance between the antenna and chip [12–14].

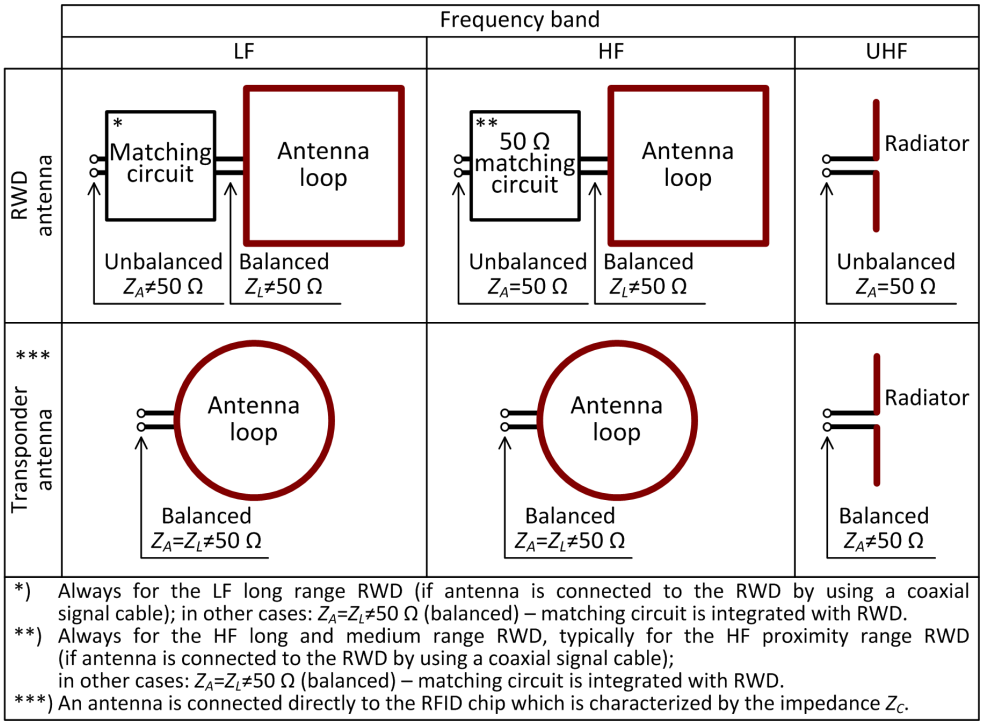

Fig. 2. Antenna constructions for RFID devices.

Radiatively coupled RFID systems in the UHF band work in the range of a far field where the emitted wave (of frequency f_0) is not only a data carrier but first of all an energy source (of power density S – Fig. 1). The electromagnetic field is always generated by the RWD. The RWD antenna together with transponder antennas comprise a radio communication arrangement that has to be wave- and impedance-matched (Fig. 2). It should be emphasized that classical impedance matching of a transmitter and receiver is established only between the RWD output and the connected antenna (50 Ω). If a transponder appears in the interrogation zone, it can be supplied with energy and the data can be exchanged but the backscattered modulation is used to send answers back to the RWD. In the transponder backscattering response the emitted wave is only partially reflected towards the RWD because of switching load impedance of the internal chip – this process is extremely power-saving but the conveyed energy is limited . The appropriate communication mechanisms are defined by ISO/IEC protocols, e.g. ISO/IEC 18000-6 (EPC Class 1 Gen 2), 18000-4 for the UHF band.

In RFID systems in the UHF band, the measurement problem concerns transponders and consists in the necessity of determining an impedance that is different from the common value of 50 Ω. This impedance can be described as:

$$Z_A = R_A + jX_A, \tag{2}$$

where R_A i X_A denote the resistance and reactance of the transponder antenna.

The antenna impedance Z_A is constant at a given frequency but the chip impedance Z_C varies with the power that is transferred from the antenna to the chip [15]. The power level changes are caused by the transponder RF front-end [16]. This characteristic is crucial in the transponder antenna synthesis. The maximum IZ of an RFID system is obtained for full impedance matching of the antenna and chip (Z_A=Z_C* at the chip sensitivity, where * indicates the complex conjugate) [17].

The above-mentioned impedance parameters determined in each of the described frequency bands (LF, HF and UHF) are essential for estimating energy and communication conditions of RFID systems. The energy conditions influence the amount of energy conveyed from the RWD to transponders. The communication conditions have an effect on efficiency of data transmission by a wireless medium.

In LF systems, the typical RLC bridge working in the given frequency band can be used for measuring parameters of antenna loops. The measurement problem is more complicated in the HF and UHF bands. Two unsymmetrical 50 Ω ports (P1, P2) of a VNA analyzer and PDP probes (Fig. 3-a) have to be used in the experimental procedure. The procedure consists in realization of an indirect differential measurement of impedance parameters: balanced Device Under Test (DUT) or Antenna Under Test (AUT) – with respect to a kind of device under test: the antenna or its part. The differential measuring technique is not applied to RWD antennas in the UHF band because the impedance is matched to the typical value of 50 Ω. It is realized by using just the one unsymmetrical port of the VNA.

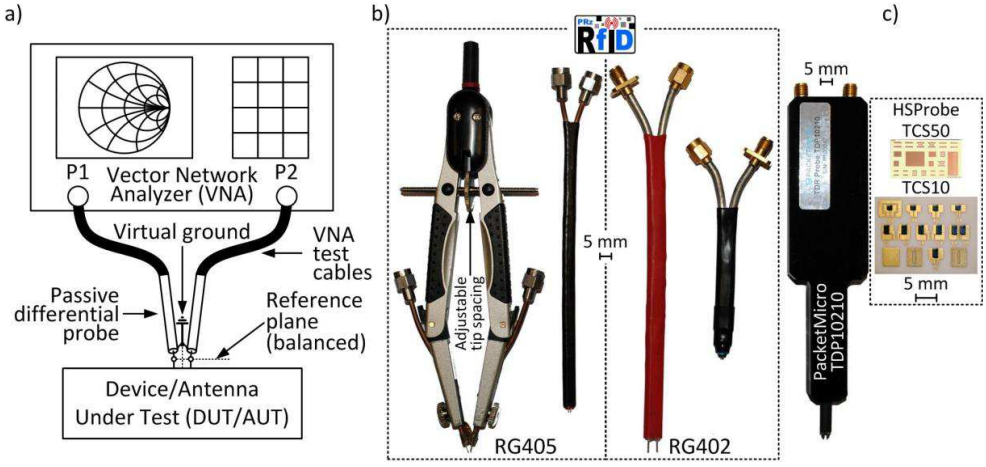

Fig. 3. Measurement setup: a) block diagram, b) examples of a passive differential probe, c) examples of calibration substrate.

Metrol. Meas. Syst., Vol. XXI (2014), No. 3, pp. 509–520.

The ports of the analyzer play the function of a signal transmitter or receiver. The function can be distinguished on the basis of an estimated scattering matrix **S** [18, 19]. The DUT/AUT separation from connection wires is provided by a differential probe. It makes possible to connect test samples to the measurement equipment. The probes should be matched to tested samples individually because of the diversity types and designs of antennas (Fig. 2) [20–22]. Depending on the requirements of conducted investigations, the probes can be realized by using two connected semi-rigid 50 Ω coaxial cables, for example 3.58 mm RG402 or 2.2 mm RG405 (Fig. 3-b). Solutions available commercially, e.g. Agilent N1021B (adjustable tip spacing from 0.5 mm to 2.54 mm) [23], Tektronix P80318 (adjustable tip spacing from 0.5 mm to 4.2 mm) [24], PacketMicro TDP102xx or TDP104xx (constant tip spacing: 0.5 mm, 0.8 mm, 1.0 mm, depending on the probe) [25] can be also applied.

The test procedure of impedance parameter determination should be performed in several steps (VNA calibration [26], measurement). In the first step, standard VNA parameter setting and calibration are conducted at the end of the test cables. Then the differential probe is connected to these cables and the port extension technique (open or short circuit) is used to shift the calibration plane to the tips of the probe (the DUT/AUT gate). In most cases, removing the DUT/AUT will leave a suitable open circuit at the new reference plane. The calibration process can be also performed in one step. It can be realized at the probe tips using a suitable calibration substrate (Fig. 3-c). After calibration, the scattering matrix **S** is measured and results are used in the impedance parameter (1) or (2) calculations. These parameters are necessary for designing efficient antennas.

3. Measurement model

3.1. Relationship between S and Z parameters

Measurements of the scattering matrix **S** do not provide immediate readout of the impedance parameters (1) or (2) in DUT/AUT cases. The final dependence of the differential impedance Z_d [27–29] can be found in the branch literature but the problem essence is never disclosed. Nevertheless, the problem is crucial in the context of measuring various antenna structures working in transponders and RWD devices in the LF, HF and UHF bands.

The typical linear two-port network is characterized by DUT/AUT parameters such as the impedance matrix **Z** or scattering matrix **S** (Fig. 4).

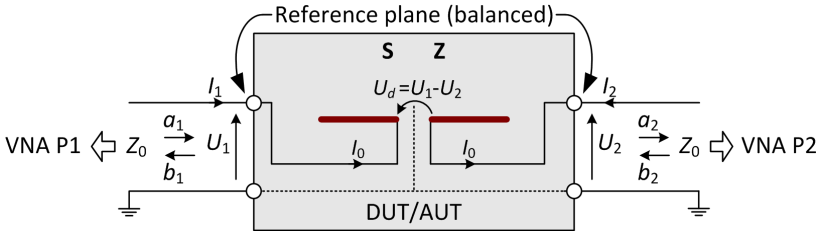

Fig. 4. Two-port network for DUT/AUT.

The impedance model describes the linear relation between U_1, U_2 voltage and I_1, I_2 input currents at the input and output correspondingly:

$$\begin{bmatrix} U_1 \\ U_2 \end{bmatrix} = \begin{bmatrix} Z_{11} & Z_{12} \\ Z_{21} & Z_{22} \end{bmatrix} \begin{bmatrix} I_1 \\ I_2 \end{bmatrix}, \tag{3}$$

where Z_{11}, Z_{12}, Z_{21}, Z_{22} are impedance parameters of matrix **Z**.

The scattering matrix **S** defines relationships between the incoming a_1, a_2 and outgoing waves b_1, b_2 (i.e. traveling wave variables):

$$\begin{bmatrix} b_1 \\ b_2 \end{bmatrix} = \begin{bmatrix} S_{11} & S_{12} \\ S_{21} & S_{22} \end{bmatrix} \begin{bmatrix} a_1 \\ a_2 \end{bmatrix}, \tag{4}$$

where S_{11}, S_{22} (reflection coefficients) and S_{21}, S_{12} (transmission coefficients) are the *S*-parameters defined as:

$$S_{11} = \left.\frac{b_1}{a_1}\right|_{a_2=0}, S_{22} = \left.\frac{b_2}{a_2}\right|_{a_1=0}, S_{21} = \left.\frac{b_2}{a_1}\right|_{a_2=0}, S_{12} = \left.\frac{b_1}{a_2}\right|_{a_1=0}. \tag{5}$$

The traveling wave variables are defined as follows:

$$a_1 = \frac{U_1 + Z_0 I_1}{2\sqrt{Z_0}}, a_2 = \frac{U_2 + Z_0 I_2}{2\sqrt{Z_0}}, b_1 = \frac{U_1 - Z_0 I_1}{2\sqrt{Z_0}}, b_2 = \frac{U_2 - Z_0 I_2}{2\sqrt{Z_0}}, \tag{6}$$

where Z_0 means the real part of the wave impedance substituted electric circuits connected to the input and output of the two-port network. An equal wave impedance Z_0=50 **Ω** is assumed for both circuits (VNA, test cables, differential probe) in the considered case.

If variables (6) are used in the model with parameters *S* (4), the matrix equation is obtained:

$$\frac{1}{2\sqrt{Z_0}}(\mathbf{U} - Z_0\mathbf{I}) = \frac{1}{2\sqrt{Z_0}}\mathbf{S}(\mathbf{U} + Z_0\mathbf{I}), \tag{7}$$

where **U** and **I** are voltage and current vectors in the two-port network. After simplification, (7) can be written as follows:

$$\mathbf{U} - Z_0\mathbf{I} = \mathbf{S}(\mathbf{U} + Z_0\mathbf{I}). \tag{8}$$

Metrol. Meas. Syst., Vol. XXI (2014), No. 3, pp. 509–520.

On the basis of the distributive property of matrix multiplication over addition and orthogonal property of the unit matrix **1**, (8) can be written as follows:

$$\mathbf{U} = Z_0(\mathbf{1}-\mathbf{S})^{-1}(\mathbf{1}+\mathbf{S})\cdot\mathbf{I}. \tag{9}$$

On the basis of (3) and (9), the direct dependence between **Z** and **S** matrix is given:

$$\mathbf{Z} = Z_0(\mathbf{1}-\mathbf{S})^{-1}(\mathbf{1}+\mathbf{S}). \tag{10}$$

After adequate transformation, the above equation can be written as follows:

$$\begin{bmatrix} Z_{11} & Z_{12} \\ Z_{21} & Z_{22} \end{bmatrix} = Z_0 \begin{bmatrix} \dfrac{(1+S_{11})(1-S_{22})+S_{12}S_{21}}{(1-S_{11})(1-S_{22})-S_{12}S_{21}} & \dfrac{2S_{12}}{(1-S_{11})(1-S_{22})-S_{12}S_{21}} \\ \dfrac{2S_{21}}{(1-S_{11})(1-S_{22})-S_{12}S_{21}} & \dfrac{(1-S_{11})(1+S_{22})+S_{12}S_{21}}{(1-S_{11})(1-S_{22})-S_{12}S_{21}} \end{bmatrix}. \tag{11}$$

The conversion of *S*-parameters into *Z* ones is possible on the basis of the carried out transformation. It is used for obtaining the differential impedance Z_d.

3.2. Differential impedance

On the basis of the typical linear two-port network which characterized a DUT/AUT (Fig. 4), the differential impedance Z_d is defined as:

$$Z_d = \frac{U_d}{I_0} = \frac{U_1 - U_2}{I_0}, \tag{12}$$

where DUT/AUT current $I_0=I_1=-I_2$.

If I_0 is put into the model (3), the equation system is obtained:

$$\begin{cases} U_1 = Z_{11}\cdot I_0 + Z_{12}\cdot(-I_0) \\ U_2 = Z_{21}\cdot I_0 + Z_{22}\cdot(-I_0) \end{cases}, \tag{13}$$

It yields the differential impedance Z_d dependent only on impedance parameters of the two-port network:

$$Z_d = (Z_{11} - Z_{12} - Z_{21} + Z_{22}). \tag{14}$$

If the dependence (11) which is used for conversing Z parameters into S-parameters is put into (14), the impedance equation is given as follows:

$$Z_d = 2Z_0 \frac{S_{12}S_{21} - S_{11}S_{22} - S_{12} - S_{21} + 1}{(1 - S_{11})(1 - S_{22}) - S_{12}S_{21}}, \tag{15}$$

This dependence can be utilized for simplifying the equation of differential impedance providing that both measuring channels are symmetrical (the test cables and the probe electrical connection lines are identical: S_{11}=S_{22}, S_{12}=S_{21}). It yields the uncomplicated solution:

$$Z_d = 2Z_0 \frac{S_{12}^2 - S_{11}^2 - 2S_{12} + 1}{(1 - S_{11})^2 - S_{12}^2}. \tag{16}$$

Finally, on the basis of (15) and (16) and also results of **S** matrix measurements (according to the arrangement presented in Figure 3-a), the impedance parameters (1) or (2) can be obtained for DUT/AUT for the given antenna type and frequency band.

4. Results

The impedance measurement problem in RFID technique is discussed on the basis of practical implementations of various antenna constructions which are made in PCB technology. The measurement results are compared with numerical data obtained for models in the Mentor Graphics HyperLynx 3D EM (HL3DEM). The investigation has been done by using the test stand in the RFID laboratory at the Department of Electronic and Communications Systems, Rzeszow University of Technology (Fig. 5).

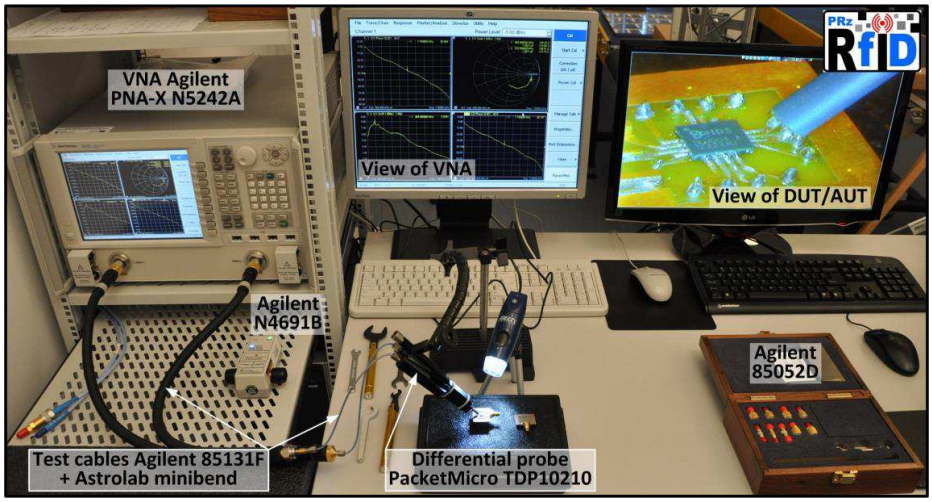

Fig. 5. Test stand in the RFID laboratory.

Metrol. Meas. Syst., Vol. XXI (2014), No. 3, pp. 509–520.

The *S*-parameters of DUT/AUT were measured by using the VNA Agilent PNA-X N5242A and the passive differential probe which has been selected according to the test antenna. This equipment was connected by flexible test cables: Agilent 85131F and Huber+Suhner (Astrolab) minibend. Firstly the stand was calibrated at the end of test cables by the electronic calibration module (Agilent N4691B) or the economy mechanical calibration kit (Agilent 85052D). Then the measurement reference plane was moved to the end of the probe tips by a port extension method [26].

The first example is the octagonal RWD antenna which is dedicated to a multiprotocol circuit of a read/write device of the proximity-range RFID system in HF band [9]. The diagram of the HL3DEM antenna model is presented in Figure 6-a. The test antenna has been realized practically on a PCB substrate by using typical FR-4 laminate (thickness 1.55 mm, dielectric constant 4.85 and loss tangent 0.025 at f=10 MHz, thickness of copper 18 μm) and is presented in Figure 6-b.

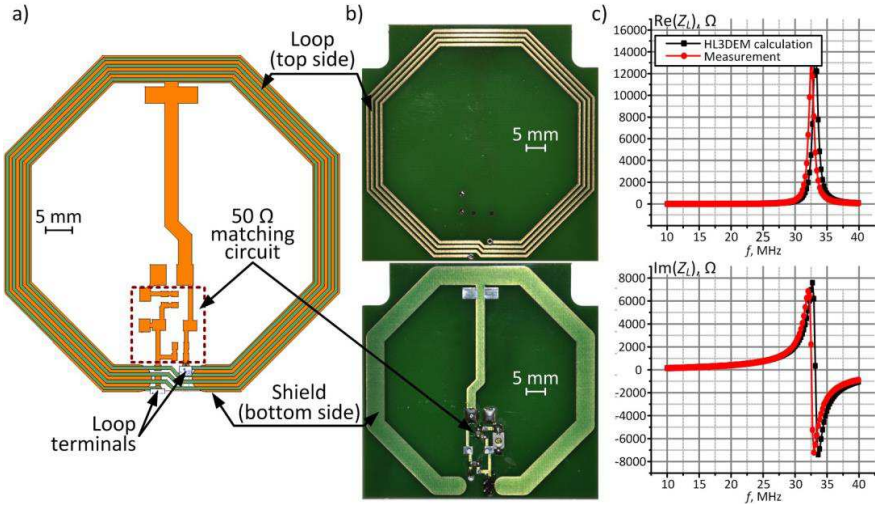

Fig. 6. Octagonal HF RWD antenna: a) design model, b) sample, c) impedance of antenna loop.

The loop impedance Z_L is presented in Figure 6-c. It has been calculated for the model and practically measured at the loop terminals by using the RG405 probe with adjustable tip spacing (Fig. 3-b) and (16) for obtaining final results. The circuit parameters which have been calculated from (1) for the operating frequency f_0=13.56 MHz are summarized in Table 1 (measurement results for antenna sample from Figure 6).

Table 1. Calculated and measured parameters of the antenna loop.

Parameter	HL3DEM calculation results	Measurement results
L_S	2.55 μH	2.51 μH
R_S	3.65 Ω	3.48 Ω

The minor discrepancies which can be seen near self-resonance (Fig. 6-c) are due to the fact that material parameters have been assumed constant in the whole frequency band in the numerical calculation. The obtained values show satisfactory convergence in order to complete the process of antenna synthesis which has been comprehensively presented in [9].

The second example is a UHF transponder antenna that is dedicated to work with the passive/semi-passive chip (IDS/AMS SL900A in QFN16 package [30]). The diagram of the

HL3DEM antenna model is presented in Figure 7-a. The test antenna (Fig. 7-b) is made on Isola FR408 laminate of 0.51 mm thick (dielectric constant 4.19 and loss tangent 0.0117 at f=1 GHz, thickness of copper 18 μm).

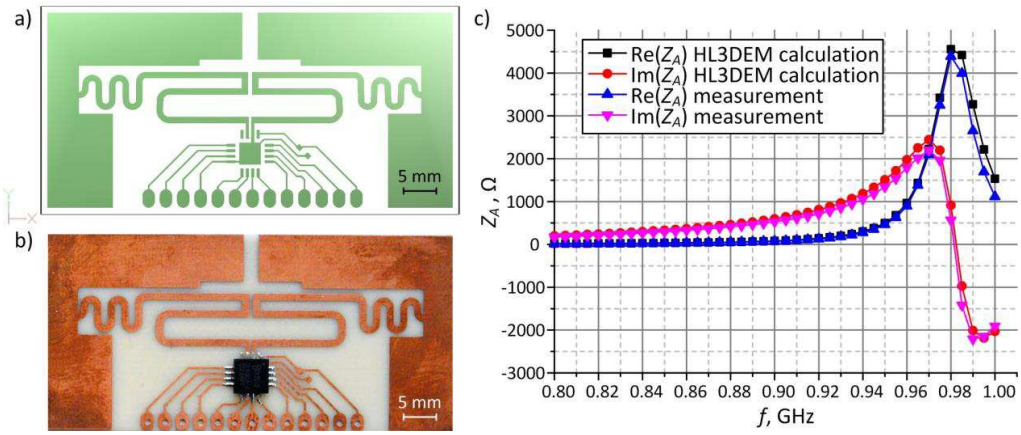

Fig. 7. Transponder antenna for UHF band: a) design model, b) sample with chip, c) impedance.

The antenna impedance Z_A is presented in Figure 7-c. It has been calculated for the model and practically measured by using the PacketMicro TDP10210 probe (Fig. 3-b) and (16) for obtaining final results.

The minor discrepancies which can be seen in Figure 7-c are due to the fact that material parameters have been assumed constant in whole frequency band in the numerical calculation. These differences also arise from the accuracy of mapping the antenna geometry in the PCB technology processes, in which the PCB plotter LPKF ProtoMat S100 has been used. The obtained values in the whole RFID UHF band (860-960 MHz) show satisfactory convergence in order to analyze the impedance matching effect between antenna and chip.

5. Conclusion

Despite popular belief, the RFID market does not offer universal systems which could be dedicated for any application in various areas of people's economical and social activities. It is the main reason why every element of the RFID system has to be designed straight for a considered implementation. This problem especially concerns antenna constructions prepared for both transponder and RWD components. As it has been shown, the experimental verification of impedance parameters is more complicated and different than it is commonly executed in classical radio communication systems (the systems in which typical matching to the 50 Ω or 75 Ω value is obvious). The above-mentioned impedance parameters determined in each of desired frequency bands (LF, HF and UHF) are essential for estimating energy and communication conditions of RFID systems. The energy conditions influence the amount of energy conveyed from RWD to transponders. The communication conditions have an effect on efficiency of data transmission in the wireless medium. The correct and efficient antenna synthesis procedure is essential for determination of 3-dimentional interrogation zone which is a basic application parameter of RFID systems.

The measured and calculated results show satisfactory convergence, so the presented procedures can be easily implemented in the design of new RFID systems.

Acknowledgements

This work was supported in part by the Polish National Centre for Research and Development (NCBR) under Grant No. PBS1/A3/3/2012. The work was developed by using the equipment purchased in the Operational Program Development of Eastern Poland 2007-2013 of the Priority Axis I Modern Economics of Activity I.3 Supporting Innovation under Grant No. POPW.01.03.00-18-012/09-00 and the Program of Development of Podkarpacie Province of The European Regional Development Fund under Grant No. UDA-RPPK.01.03.00-18-003/10-00.

References

[1] Finkenzeller, K. (2010). *RFID Handbook*. 3-rd ed., Wiley.

[2] Yao, W., Chu, C.H., Li, Z. (2012). The Adoption and Implementation of RFID Technologies in Healthcare: A Literature Review. *J. Med. Syst*., 36, 3507–3525.

[3] Costa, C., Antonucci, F., Pallottino, F., Aguzzi, J., Sarriá, D., Menesatti, P. (2013). A Review on Agri-food Supply Chain Traceability by Means of RFID Technology. *Food Bioprocess Technol.*, 6, 353–366.

[4] Ha, O., Park, M., Lee, K., Park, D. (2013). RFID Application in the Food-Beverage Industry: Identifying Decision Making Factors and Evaluating SCM Efficiency. *KSCE Journal of Civil Engineering*, 7, 1773–1781.

[5] Ustundag, A. (2013). *The Value of RFID, Benefits vs. Costs*. Springer-Verlag.

[6] Jankowski-Mihułowicz, P., Węglarski, M. (2012). Determination of 3-Dimentional Interrogation Zone in Anticollision RFID Systems with Inductive Coupling by Using Monte Carlo Method. *Acta Phys. Pol. A*, 121(4), 936–940.

[7] Sharma, A., Zuazola, I.J.G., Gupta, A., Perallos, A., Batchelor, J.C. (2013). Non-Uniformly Distributed-Turns Coil Antenna for Enhanced H-Field in HF-RFID. *IEEE Trans. Antennas Propag.*, 61(10), 4900–4907.

[8] Petrariu, A.-I., Popa, V., Gaitan, V.-G., Finis, I. (2012). Test results for HF RFID antenna system tuning in metal environment. In *Proc. of 13th ICCC 2012*. High Tatras, Slovakia, 543–546.

[9] Jankowski-Mihułowicz, P., Węglarski, M. (2012). Synthesis of Read/Write Device Antenna for HF Proximity Range RFID Systems with Inductive Coupling. *PE*, 88(3a), 70–73.

[10] Ahmad, M.Y., Mohan, A.S. (2011). Multi-loop bridge HF RFID reader antenna for improved positioning. In *Proc. of APMC 2011*. Melbourne, Australia, 1426–1429.

[11] Qing, X., Chen, Z.N. (2009). Characteristics of a metal-backed loop antenna and its application to a high-frequency RFID smart shelf. *IEEE Antennas Propag. Mag.*, 51(2), 26–38.

[12] Wobak, M., Gebhart, M., Muehlmann, U. (2012). Physical Limits of Batteryless HF RFID Transponders defined by System Properties. In *Proc. IEEE RFID-TA 2012*. Grenoble, France, 142–147.

[13] Ohnimus, F., Ndip, I., Guttowski, S., Reichi, H. (2008). Design and analysis of a bent antenna-coil for a HF-RFID transponder. In *Proc. 38th Eur. Microw. Conf. 2008*. Amsterdam, Netherlands, 75–78.

[14] Hennig, A. (2008). Feasibility of Deeply Implanted Passive Sensor Transponders in Human Bodies. In *Proc. of 4th European Workshop on RFID SysTech 2008*. Freiburg, Germany, 1–7.

[15] De Vita, G., Iannaccone, G. (2005). Design criteria for the RF section of UHF and microwave passive RFID transponders. *IEEE Trans. Microw. Theory Tech.*, 53(9), 2978–2990.

[16] Wei, P., Che, W., Bi, Z., Wei, C., Na, Y., Qiang, L., Hao, M. (2011). High-Efficiency Differential RF Front-End for a Gen2 RFID Tag. *IEEE Trans. Circuits Syst.*, 58(4), 189–194.

[17] Dobkin, D. (2012). *The RF in RFID, UHF RFID in Practice*, SE. Newnes, 2012.

[18] Meyers, R., Janssens, F. (1998). Measuring the impedance of balanced antennas by an S-Parameter method. *IEEE Antennas and Propag. Mag.*, 40(6), 62–65.

[19] Bockelman, E., Eisenstadt, W.R. (1995). Combined Differential and Common-Mode Scattering Parameters: Theory and Simulation. *IEEE Trans. Microw. Theory Techn.*, 43(7), 1530–1539.

[20] Janeczek, K., Jankowski-Mihułowicz, P., Jakubowska, M., Kozioł, G., Młożniak, A., Futera, K., Stęplewski, W. (2012). Performance Characterization of UHF RFID Antennas Manufactured with Screen Printing Technique on Flexible Substrates. *Microelectronic Materials and Technologies*, 232(2), 61–74.

[21] Koskinen, T., Rajagopalan, H., Rahmat-Samii, Y. (2009). Impedance measurements of various types of balanced antennas with the differential probe method. In *Proc. of IEEE iWAT 2009*. Santa Monica, CA, USA, 1–4.

[22] Pantoja, A.J.J, Pena, N.M., Roman, F., Vega, F., Rachidi, F. (2012). Wideband experimental characterization of differential antenna. In *Proc. of 6th EUCAP 2012*. Prague, Czech Republic, 2135–2139.

[23] N1021B 18 GHz Differential TDR Probe Kit. Agilent, 5990-4013EN. *http://www.home.agilent.com*. (5 Nov. 2013).

[24] Differential Impedance TDR Probes for the DSA8300, P80318. Tektronix, 85W-18863-2. *http://www.tek.com*. (28 Apr. 2011).

[25] TDR BladeProbe, Innovative TDR Handheld Probe Solutions. PacketMicro, Datasheet. *http://www.packetmicro.com*. (2013).

[26] Rumiantsev, A., Ridler, N. (2008). VNA calibration, *IEEE Microw. Mag.*, 9(3), 86–99.

[27] Qing, X., Chean, K.G., Chen, Z.N. (2009). Impedance characterization of RFID tag antennas and application in tag co-design. *IEEE Trans. Microw. Theory Techn.*, 57(5), 1268–1274.

[28] Zhu, H.L., Ko, Y.C.A., Ye, T.T. (2010). Impedance measurement for balanced UHF RFID tag antennas. In *Proc. of IEEE RWS 2010*. New Orleans, LA, USA, 128–131.

[29] da Costa, F.C., de Lima, E.R., Yoshioka, R.T., Bertuzzo, J.E., Koeppe, J. (2013). Impedance measurement of dipole antenna for EPC Global compliant RFID tag. In *Proc. of SBMO/IEEE MTT-S IMOC 2013*. Rio de Janeiro, RJ, Brazil, 1–5.

[30] SL900A Single-Chip EPC Data Logger with Sensor. IDS Microchip AG, Product Flyer. *http://www.ams.com*. (March 2010).